

ENC-2020-0456

**THE INFLUENCE OF DELTA WINGLET VORTEX GENERATOR  
POSITION AND ROLL ANGLE ON FIN-AND-ELLIPTICAL TUBE HEAT  
EXCHANGER PERFORMANCE**

**Tatiana Silva Ferreira**  
**Jurandir Itizo Yanagihara**

Department of Mechanical Engineering, Polytechnic School, University of São Paulo, São Paulo, SP, Brazil  
tatianaf.94@usp.br  
jiy@usp.br

**Abstract.** *The analysis of new configurations for compact heat exchangers is important to improve their overall efficiency. This research objective is to numerically evaluate heat transfer and pressure drop in two rows of a fin-and-oval tube heat exchanger with delta winglet longitudinal vortex generators (LVGs). Oval tubes are still considered a non-conventional geometry and there are relatively few heat transfer enhancement studies connected to LVGs. Particularly, this is the first work to consider the influence of the roll angle on heat transfer enhancement in this kind of geometry. The flow analysis is performed using a commercial computational fluid dynamics software, based on the finite volume method. The Reynolds number is 1000, based on the hydraulic diameter, for a turbulent, incompressible, constant property, steady-state flow. The influence of different vortex generator positions and roll angles on heat transfer and pressure drop is analyzed. A performance evaluation criterion is used to select the best combination of the LGV geometric parameters. A thorough phenomenological analysis is also performed to clarify the heat transfer enhancement mechanism.*

**Keywords:** *Heat transfer, Heat exchanger, Elliptical tube, Thermal-hydraulic performance, Pressure drop*

## 1. INTRODUCTION

Compact heat exchangers (CHEs) are found in different engineering fields. It is possible to find them being used in many industries, such as automotive, chemical, refrigeration and even in the electronic industry to improve the cooling of small electronic devices.

Improving the overall thermal-hydraulic performance of CHEs has long been a subject of studies, since a best performance is necessary to reduce the volume of a heat exchanger. Industries such as automotive and electronic depend on reduced size and weight of CHEs for new technologies development. For that, many heat transfer techniques can be applied.

Longitudinal Vortex Generators (LVGs) are small devices, responsible for generating longitudinal vortex in a flow. Since no external power is usually required in the use of LVGs, the enhancement techniques associated with them are mostly passive. They are able to enhance heat transfer through boundary layer thinning (Yanagihara and Torii, 1992), swirl and flow destabilization (Fiebig, 1995). The addition of an LVG in a compact heat exchanger is responsible for a small increase in the total heat transfer area, but the local Nusselt number augmentation can be up to 200%, as presented by Jacobi and Shah (1995).

LVGs have long been studied (Jacobi and Shah, 1995) for different applications (Chomdee and Kiatsiriroat, 2007). They have different geometries and parameters that can influence the heat transfer enhancement they are able to provide, such as height, attack angle and aspect ratio (Yanagihara and Torii, 1992).

Among the existing studies for heat exchangers with circular tubes, there are many interesting results concerning the use of LVGs. As ? shows, LVGs can be positioned upstream of the tube, in the common-flow-up position, accelerating the flow around the tube and delaying separation. They can also be positioned downstream of the tube, in the common-flow-down position, as proposed by Fiebig *et al.* (1993), forcing the flow into the wake region. Both strategies have been proven able to enhance thermal-hydraulic performance.

Another way to improve thermal-hydraulic performance is through heat exchanger geometry change. Circular tubes are the most usual geometry, but elliptical and oval tubes can help reduce pressure loss with minor changes in the overall CHE geometry. Pooranachandran *et al.* (2015) and Du *et al.* (2013) studied elliptical tubes for different applications. Fullerton and Anand (2010) compared circular and oval tubes in compact heat exchangers and concluded that, although the heat exchange is higher with circular tubes, because of the pressure drop, oval tubes present a better thermal-hydraulic

performance. That phenomenon is explained by Gholami *et al.* (2019), proving that an elliptical tube retards the boundary layer separation and therefore reduces the wake region behind the tube. Since the elliptical and oval geometries are able to reduce pressure loss and, consequently, augment thermal-hydraulic performance, the geometry change is a suitable passive enhancement technique.

Since the use of LVGs and oval and elliptical tubes are able to improve the heat exchanger thermal-hydraulic performance, studying the effects of both techniques combined is important. Chen *et al.* (1998) analysed different configurations to understand the flow. Their study tests different numbers of LVGs, in different positions, making it possible to also visualize the vortex merge when more than one vortex generator was used. One main conclusion obtained by Chen *et al.* (1998) is that an aspect ratio of 2, commonly used for delta-winglet vortex generators, is the one with the highest thermal-hydraulic performance. Pérez *et al.* (2016), in an experimental study, show how the position of LVGs influences heat transfer in finned elliptical tube and Yanagihara *et al.* (2005) discuss the mechanisms involved in the heat transfer enhancement in the parametric study of finned oval tube with LVGs and, based on local heat transfer experiments.

All the studies support the conclusion that the use of LVGs in a CHE with elliptical tubes can improve the thermal-hydraulic performance. Different parameters have been analysed, but there is still no research on the influence of the LVG roll angle. Salviano *et al.* (2016) show that the roll angle is responsible for changes in performance. Thus, this work intends to understand the influence of this parameter on the heat transfer and pressure drop in CHE with elliptical tubes.

## 2. Methodology

### 2.1 Governing Equations

The geometrical and operational parameters adopted in the present research is based on an experimental work, developed by Pérez (2001). A three-dimensional, steady-state, turbulent and incompressible flow with constant physical properties is considered for the numerical simulations. Air, the fluid selected for this analysis, is Newtonian and presents constant properties. The selected turbulence model is the  $k-\omega$  SST and a commercial software based on the Finite Volume Method is selected to solve the mass, momentum and energy conservation equations, respectively presented below:

$$\frac{\partial(\rho u_i)}{\partial x_i} = 0 \quad (1)$$

$$\frac{\partial(\rho u_i u_j)}{\partial x_i} = -\frac{\partial p}{\partial x_j} + \frac{\partial}{\partial x_i} \left( \mu \frac{\partial u_j}{\partial x_i} \right) \quad (2)$$

$$\frac{\partial(\rho u_i T)}{\partial x_i} = \frac{\partial}{\partial x_i} \left( \alpha \frac{\partial u_j}{\partial x_i} \right) \quad (3)$$

The pressure-velocity coupling algorithm used here was the so-called Coupled algorithm, which solves the pressure-based mass conservation and the momentum equations together, and the discretization scheme was the Second-Order Upwind.

To ensure convergence, several criteria were adopted. The first was mass flux imbalance lower than 0.01%. The second was making continuity residual lower than  $10^{-3}$ , momentum residuals lower than  $10^{-6}$  and energy residual lower than  $10^{-8}$ . The last criterion was checking the key variables convergence. The variables selected were pressure and temperature averages at the outlet.

### 2.2 Thermal-Hydraulic Parameters

The analysis of thermal-hydraulic parameter is essential to verify the overall augmentation of heat transfer and pressure drop. Those parameters are calculated for each geometry and later compared to determine which of the tested geometries has a better thermal-hydraulic performance.

The parameters used to describe the flow thermal-hydraulic behavior are Reynolds Number (Re), Nusselt Number (Nu) and friction factor (f), as follows:

$$Re = \frac{u_c D_h}{\nu_{air}} \quad (4)$$

$$Nu = St Re Pr \quad (5)$$

$$f = \frac{2\Delta p A_c}{\rho u_c^2 A_o} \quad (6)$$

where  $D_h$  is the hydraulic diameter for the minimum flow area,  $u_c$  is the maximum flow velocity and Pr is the air Prandtl number. The log-mean temperature difference, total heat transfer, heat transfer coefficient, Stanton number and pressure

difference are respectively defined as:

$$\Delta T_{ln} = \frac{(T_{tubo} - \bar{T}_{in}) - (T_{tubo} - \bar{T}_{out})}{\ln \left[ \frac{T_{tubo} - \bar{T}_{in}}{T_{tubo} - \bar{T}_{out}} \right]} \quad (7)$$

$$Q = mc_p \Delta T_{ln} \quad (8)$$

$$h = \frac{Q}{A \Delta T_{ln}} \quad (9)$$

$$St = \frac{h}{\rho_{air} u_c c_p} \quad (10)$$

$$\Delta p = \bar{p}_{inlet} - \bar{p}_{outlet} \quad (11)$$

where:

$$\bar{T} = \frac{\int \int_A u T dA}{\int \int_A u dA} \quad (12)$$

$$\bar{p} = \frac{\int \int_A p dA}{\int \int_A dA} \quad (13)$$

### 2.3 Boundary Conditions and Computational Domain

The tested geometry was generated based on the geometries tested by Pérez (2001) which used the naphthalene sublimation technique to measure the heat transfer coefficient by heat and mass transfer analogy. The problem to be simulated is a flow between two aluminum plates with elliptical tubes. The main domain was extended one time at the inlet and two times at the outlet, to ensure a fully developed flow. The fully developed flow was verified in different planes to guarantee the boundary condition at the outlet was being applied correctly. The main domain is model of a real air conditioning heat exchanger, replacing circular tubes with elliptical ones. From to Figure 1, the domain dimensions are  $SL/D2 = 3.25$ ,  $D2 = 7.14$  cm,  $D1 = 14.29$  cm,  $ST/D2 = 1.75$ ,  $L = 46.43$  cm and  $E = 1.86$  cm. The air properties used in the simulation are inlet temperature of 15 C, cinematic viscosity of  $16.84 \cdot 10^{(-6)} m^2/s$ ,  $1.1774 kg/m^3$  as density and 90 C as fin temperature.

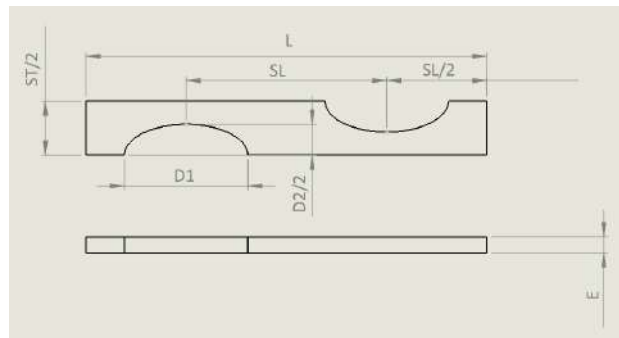


Figure 1. Model dimension

In order to perform the numerical validation and a comparative study, two different LVG position configurations were selected. Figure 2 and Table 1 present coordinate references, LVG position and LVG attack angle.

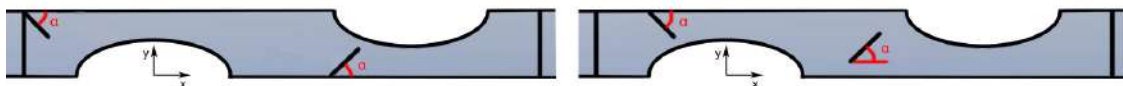


Figure 2. Configurations 1 and 2 with coordinate references

Table 1. Longitudinal Vortex Generators Positions

	X - 1st LVG	Y - 1st LVG	$\alpha - 1stLVG$	X - 2nd LVG	Y - 2nd LVG	$\alpha - 2ndLVG$
Configuration 1	-SL/2	ST/2	45	2.24 D2	0	-45
Configuration 2	-D1/2	ST/2	45	1.57 D2	0.2 D2	-45

The boundary conditions applied to the problem were selected based on the experiment performed by Pérez (2001). Different boundary conditions were applied to different surfaces, according to Figure 3.

- Inlet: constant velocity and pressure
- Outflow: null gradients for all variables
- Top and bottom walls: no slip condition and constant temperature
- Tubes and LVGs: no slip condition and adiabatic
- Side planes: symmetry
- Extended regions: symmetry

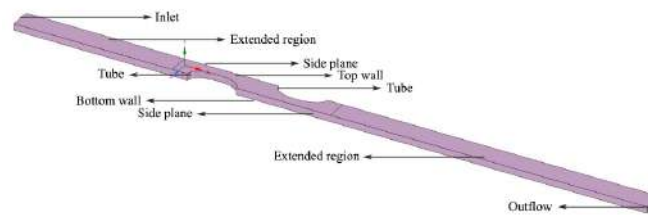


Figure 3. Boundary conditions

### 3. Grid Independence and Numerical Validation

To ensure the results are independent from the generated mesh, the Grid Convergence Index (GCI) method, as presented by Celik *et al.* (2008), is applied. The method is used for both the numerical validation and the main simulations: therefore, six different meshes were tested: three for the base case without LVGs, and three for the first LVG configuration.

The dimensionless wall distance ( $y^+$ ) was monitored for each grid to ensure the chosen turbulence model ( $k-\omega$  SST) would be able to achieve valid results. According to Ansys (2010),  $y^+$  must be as close to 1 as possible, and, if not possible, the first cell must fit inside the viscous sublayer, that is  $y^+$  must be lower than 5. Another monitored mesh parameter was the orthogonal quality, which, according to Ansys (2010), must be above 0.01.

Table 2 was built based on the procedure proposed by Celik *et al.* (2008).

Table 2. Mesh characteristics

	Grid 1 - Base	Grid 2 - Base	Grid 3 - Base	Grid 1 - LVG	Grid 2 - LVG	Grid 3 - LVG
Refinement factor	-	1.98	2.03	-	2	1.99
Maximum $y^+$	0.79	0.79	0.50	0.95	0.95	0.94
Number of elements	1679097	3317055	6752212	1802421	3613273	7190459
Nu	5.65	5.42	5.41	7.2342	7.1346	7.1500
f	0.193	0.190	0.189	0.0352	0.368	0.037

For the base case, there is a calculated numerical error of approximately 0.2125% for the fine grid and 4.7% for the intermediate grid. The same procedure is applied to the LVG case. The fine grid presents a numerical error of approximately 0.2154% and the intermediate 1.377%. The GCI for the base case is 1.02 and for the LVG case, 0.9884: both are close to 1. The grid independence is checked for both cases and the intermediate grid is selected as a mesh density reference.

To validate the numerical procedure, different Reynolds numbers were applied to Configuration 2 and Nusselt number and friction factor were compared to the ones for the base case. The results were compared to the ones in Pérez (2001).

Figure 4 shows the comparison. The results show that the thermal-hydraulic behavior is consistent with the experimental results: therefore, the numerical simulations here presented are reliable.

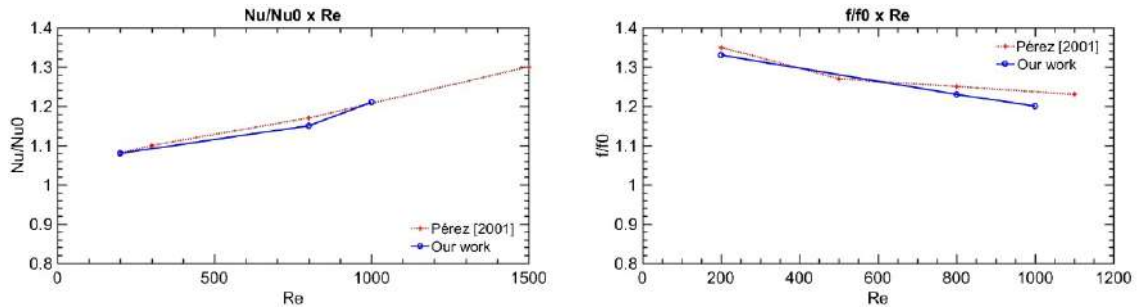


Figure 4. Comparison for our work and Pérez (2001)

#### 4. Results and Discussions

In order to analyse the influence of LVG roll angle ( $\phi$ ) in the heat transfer and pressure drop in a CHE with elliptical tubes, four different angles were selected and tested. The angle was concurrently applied to both LVGs.

##### 4.1 Flow Analysis

Figure 5 shows the velocity field at 5.9 mm height for Configuration 1. Figure 6 shows the velocity field at the same location for Configuration 2.

It is noticeable that the position of the vortex generator influences the velocity around the tube. In Configuration 1, the first LVG is further from the tube than in Configuration 2 and, consequently, the velocity around the first tube is increased in Configuration 2. The same behavior is observed in the second LVG. The change in the velocity around the tube delays separation and reduces the wake region. That is specially noticed in Configuration 2.

Since the LVG is an obstacle in the flow, there is naturally a wake region behind it. The results show an augmentation in this region as the roll angle reduces. Another remark is the influence of the second LVG's roll angle in the wake region behind the first tube. In Configuration 2, it is possible to see that, as the roll angle decreases, the wake region also is reduced.

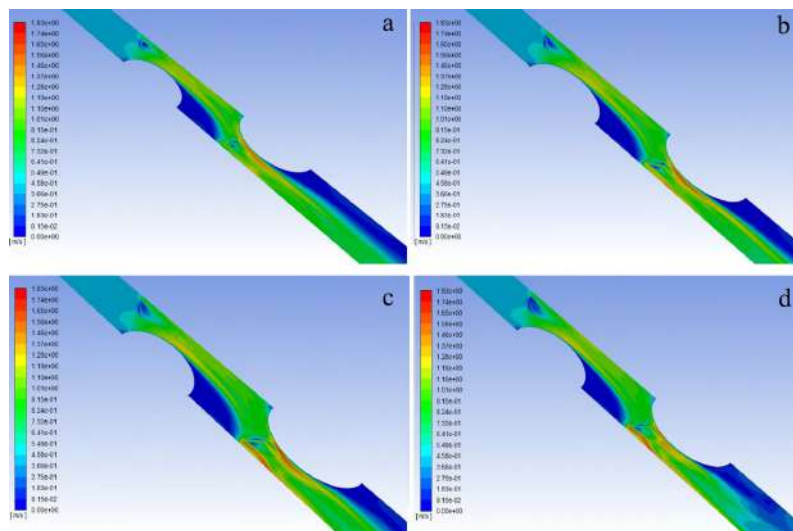


Figure 5. Velocity field in the first configuration of LVGs for a)  $\phi = 45^\circ$  b)  $\phi = 30^\circ$  c)  $\phi = 15^\circ$  d)  $\phi = 0^\circ$

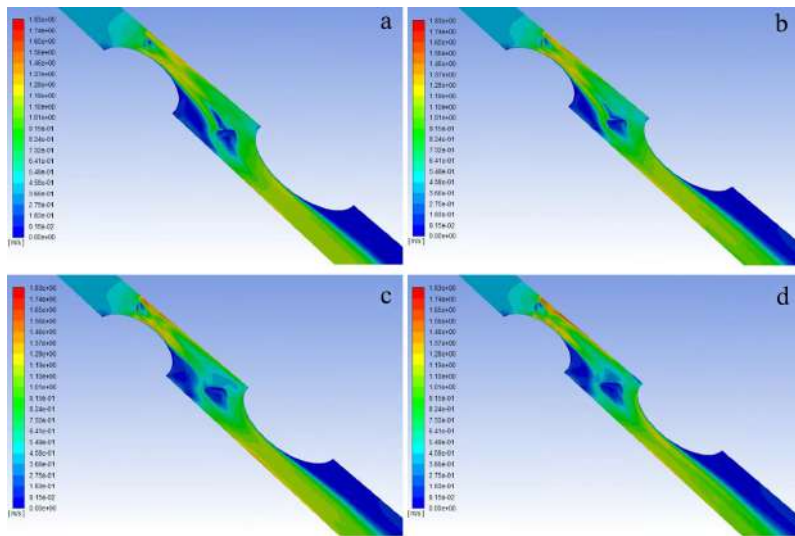


Figure 6. Velocity field in the second configuration of LVGs for a)  $\phi = 45$  b)  $\phi = 30$  c)  $\phi = 15$  d)  $\phi = 0$

Figures 7 and 8 show the flow field after the first LVG in the first and second LVGs configuration. The first plane is 3.72 cm away from the heat exchanger inlet and the second is 7.72 cm for Configuration 1. For Configuration 2 plane 1 is 8.20 cm away from the heat exchanger inlet and plane 2 is 12.20 cm away.

The vortex generated is clearly stronger as the roll angle decreases. The position of the LVG also influences, as the second configuration has the LVG closer to the tube and the vortex takes longer to dissipate.

Figures 7 and 8 show the flow field after the first LVG in the first and second LVGs configuration ( $x_1 = 31.0$  cm and  $x_2 = 34.0$  cm for Configuration 1 and  $x_1 = 26.20$  cm and  $x_2 = 30.20$  cm for Configuration 2).

The behavior observed in the first LVG repeats itself in the second LVG, whereby vortices take longer to dissipate in the cases with smaller roll angles.

All the results from the flow field analysis confirm the enhancement mechanisms presented. Figures 5 to 10 show the boundary layer thinning and the mixing in the wake region. Those mechanisms are expected to increase the heat transfer enough to compensate for the increase in pressure drop.

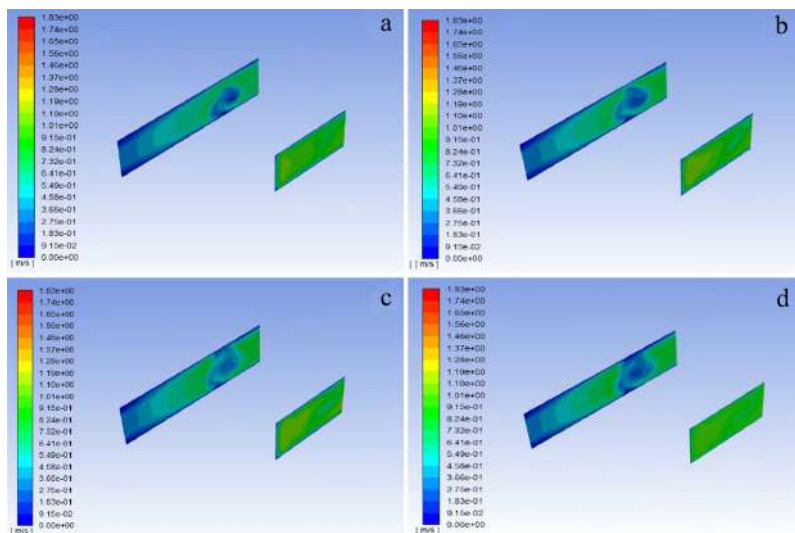


Figure 7. Flow field in Configuration 1 after the first LVG for a)  $\phi = 45$  b)  $\phi = 30$  c)  $\phi = 15$  d)  $\phi = 0$

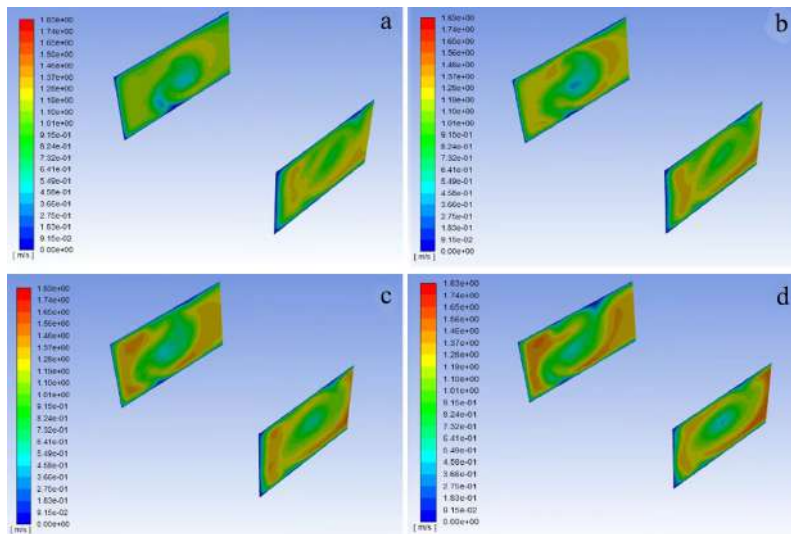


Figure 8. Flow field in Configuration 2 after the first LVG for a)  $\phi = 45$  b)  $\phi = 30$  c)  $\phi = 15$  d)  $\phi = 0$

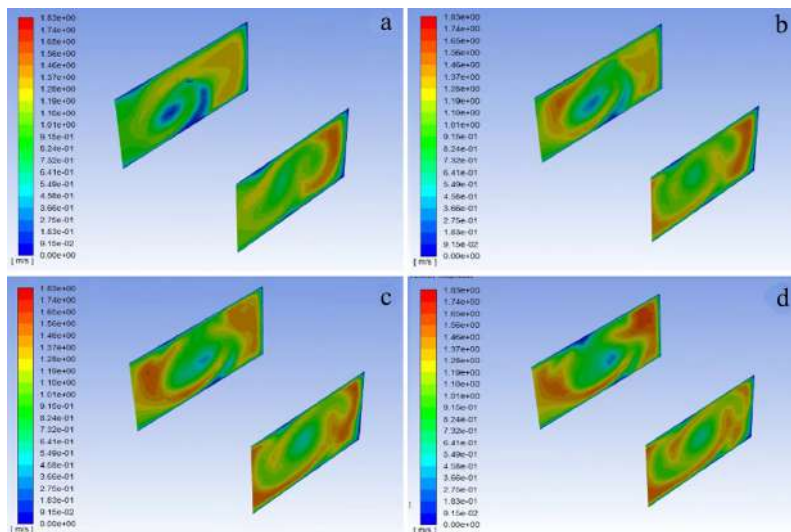


Figure 9. Flow field in Configuration 1 after the second LVG for a)  $\phi = 45$  b)  $\phi = 30$  c)  $\phi = 15$  d)  $\phi = 0$

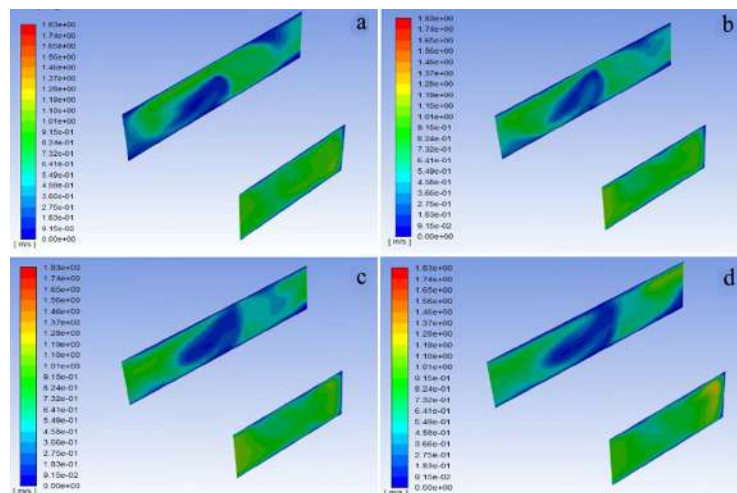


Figure 10. Flow field in Configuration 2 after the second LVG for a)  $\phi = 45$  b)  $\phi = 30$  c)  $\phi = 15$  d)  $\phi = 0$

## 4.2 Heat Transfer

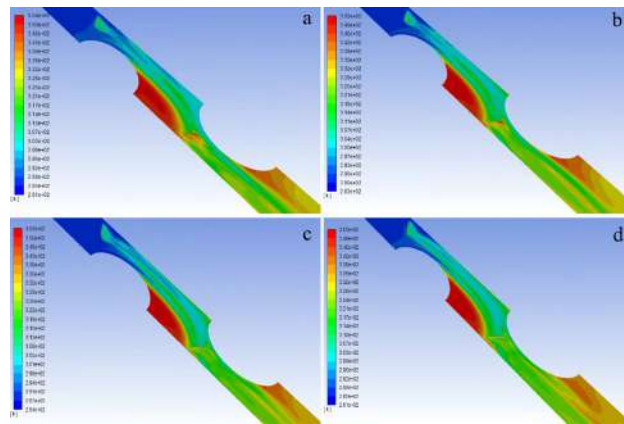


Figure 11. Temperature field in Configuration 1 for a)  $\phi = 45^\circ$  b)  $\phi = 30^\circ$  c)  $\phi = 15^\circ$  d)  $\phi = 0^\circ$

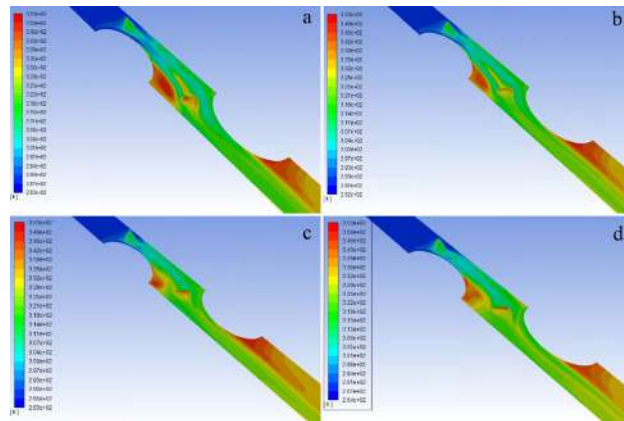


Figure 12. Temperature field in Configuration 2 for a)  $\phi = 45^\circ$  b)  $\phi = 30^\circ$  c)  $\phi = 15^\circ$  d)  $\phi = 0^\circ$

The temperature field for Configurations 1 and 2 at 5.9 mm height is shown, respectively, in Figures 11 and 12.

Those results show the reduction in the wake region behind the first tube, influenced by the second LVG and by the increased velocity around the tube. This reduction is more evident in the second case, since both vortex generators are closer to the tube, and is directly affected by the roll angle; reductions in the roll angle reduce the wake region.

The global Nusselt number was calculated and is presented in Figure 13.

The results show that a smaller roll angle increases heat transfer when compared to the base case. This behavior was expected, since the vortex generated in those configurations takes longer to dissipate and the enhancement mechanisms are more intense. Also, the wake region behind the tube is reduced by a smaller roll angle, which also improves heat transfer.

The second configuration presented a higher Nusselt number for all the roll angles. This is explained by the vortex effects, which are more intense in Configuration 2, thus intensifying even more the heat transfer enhancement.

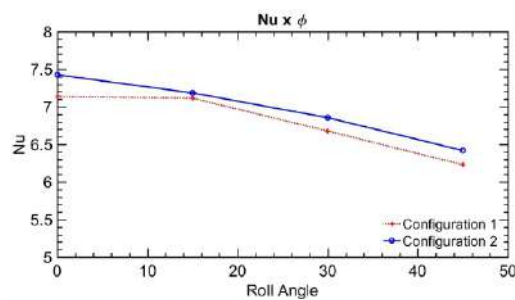


Figure 13. Global Nusselt number (Nu) for different LVG configurations and roll angles ( $\phi$ )

### 4.3 Pressure Drop

The calculated friction factor is presented in Figure 14.

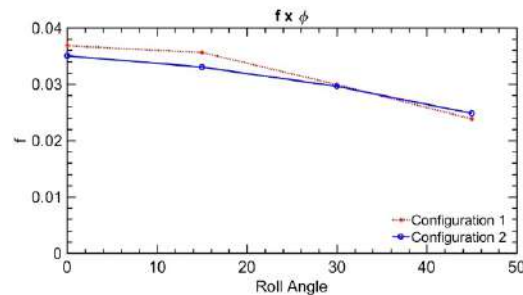


Figure 14. Friction factor (f) for different LVG configurations and roll angles ( $\phi$ )

As expected, the friction factor decreases with higher roll angles. Since the LVG is a flow obstacle, increasing the roll angle creates a smoother path to the flow and the pressure drop will be smaller. However, note that, for the friction factor, the difference between the two configurations is small. Configuration 2 is better for the two first roll angles. For  $\phi = 30$ , Configuration 1 and 2 are nearly equal and, for  $\phi = 45$ , Configuration 1 has a smaller friction factor.

### 4.4 Thermal-Hydraulic Performance

To evaluate the thermal-hydraulic performance, parameter R, as defined by Pérez (2001) was used:

$$R = \frac{\frac{Nu}{Nu_0}}{\frac{f}{f_0}} \quad (14)$$

Figure 15 shows the R values in each configuration and roll angle.

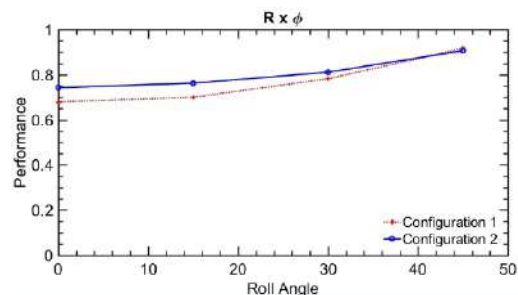


Figure 15. Thermal-hydraulic performance for different LVG configurations and roll angles ( $\phi$ )

It is noticeable that, even though heat transfer is higher with smaller roll angles, the overall thermal-hydraulic performance increases with higher roll angles, due to the influence of pressure drop.

The best thermal-hydraulic performance was from Configuration 1 with  $\phi = 45$ . This analysis is important to understand that the use of roll angle in LVGs can generate geometries that will achieve higher performances.

Further study is still necessary to check different roll angles and geometries in order to find better configurations.

### 5. Conclusion

A numerical analysis of heat transfer and pressure drop in two rows of a fin-and-oval tube heat exchanger with delta winglet longitudinal vortex generators (LVGs) was performed. The influence of different vortex generator positions and roll angles on heat transfer and pressure drop was evaluated. The major findings in this research were:

- LVG roll angle and position influence heat transfer and pressure drop.
- A smaller roll angle increases heat transfer and pressure drop.
- Thermal-hydraulic performance increases with higher roll angles.
- Between the two different configurations evaluated, Configuration 1 with  $\phi = 45$  had the best thermal-hydraulic performance.

- To find the best LVG configuration, the LVG roll angle must be taken into consideration, since its influence on pressure drop can be significant towards thermal-hydraulic performance evaluation.

## 6. ACKNOWLEDGEMENTS

The first author would like to acknowledge Coordenação de Aperfeiçoamento de Pessoal de Nível Superior (Capes - Brazilian Coordination for the Improvement of Higher Education Personnel) for the financial support. The second author would like to acknowledge CNPq (Brazilian National Council for Scientific and Technological Development) for research grant 309214/2017-3.

## 7. REFERENCES

- Ansys, 2010. *Ansys Fluent User's Guide*. Ansys, INC.
- Celik, I.B., Ghia, U., Roache, P.J., Freitas, C.J., Coleman, H. and Raad, P.E., 2008. "Procedure for estimation and reporting of uncertainty due to discretization in cfd applications". *Journal of Fluids Engineering*, Vol. 130, No. 7, p. 078001. doi:10.1115/1.2960953.
- Chen, Y., Fiebig, M. and Mitra, N.K., 1998. "Conjugate heat transfer of a finned oval tube with a punched longitudinal vortex generator in a form of a delta winglet - parametric investigation of the winglet". *International Journal of Heat and Mass Transfer*, Vol. 41, No. 23, pp. 3961–3978.
- Chomdee, S. and Kiatsiroat, T., 2007. "Air-cooling enhancement with delta winglet vortex generators in entrance region of in-line array electronic modules". *Heat Transfer Engineering*, Vol. 28, No. 4, pp. 372–379. doi:10.1080/01457630601123003.
- Du, X., Zeng, M., Wang, Q. and Dong, Z., 2013. "Experimental investigation of heat transfer and resistance characteristics of a finned oval-tube heat exchanger with different air inlet angles". *Heat Transfer Engineering*, Vol. 35, No. 6-8, pp. 703–710. doi:10.1080/01457632.2013.837780.
- Fiebig, M., 1995. "Embedded vortices in internal flow: heat transfer and pressure loss enhancement". *International Journal of Heat and Fluid Flow*, Vol. 16, No. 5, pp. 376–388.
- Fiebig, M., Valencia, A. and Mitra, N.K., 1993. "Wing-type vortex generators for fin-and-tube heat exchangers". *Experimental Thermal and Fluid Science*, Vol. 7, No. 4, pp. 287–295.
- Fullerton, T.L. and Anand, N.K., 2010. "Periodically fully-developed flow and heat transfer over flat and oval tubes using a control volume finite-element method". *Numerical Heat Transfer, Part A: Applications*, Vol. 57, No. 9, pp. 642–665. doi:10.1080/10407781003744888.
- Gholami, A., Mohammed, H.A., Wahid, M.A. and Khiadani, M., 2019. "Parametric design exploration of fin-and-oval tube compact heat exchangers performance with a new type of corrugated fin patterns". *International Journal of Thermal Sciences*, Vol. 144, pp. 173–190. doi:10.1016/j.ijthermalsci.2019.05.022.
- Jacobi, A.M. and Shah, R.K., 1995. "Heat transfer surface enhancement through the use of longitudinal vortices: a review of recent progress". *Experimental Thermal and Fluid Science*, Vol. 11, No. 3, pp. 295–309.
- Pooranachandran, K., Ali, K., Narasingamurthi, K. and Ramalingam, V., 2015. "Experimental and numerical investigation of a louvered fin and elliptical tube compact heat exchanger". *Thermal Science*, Vol. 19, No. 2, pp. 679–692. doi:10.2298/tsci120220146p.
- Pérez, R.B., Yanagihara, J.I. and Bayon, J.J.G., 2016. "An experimental study of heat transfer enhancement using vortex generators in a finned elliptical tube". *Ingeniería Energética*, Vol. 37, pp. 165–175.
- Pérez, R.B., 2001. *Análise experimental da intensificação da transferência de calor através de geradores de vórtices em trocadores de calor compactos com tubos de geometria elíptica*. Ph.D. thesis, Universidade de São Paulo.
- Salviano, L.O., Dezan, D.J. and Yanagihara, J.I., 2016. "Thermal-hydraulic performance optimization of inline and staggered fin-tube compact heat exchangers applying longitudinal vortex generators". *Applied Thermal Engineering*, Vol. 95, pp. 311–329. doi:10.1016/j.applthermaleng.2015.11.069.
- Yanagihara, J.I., Pérez, R.B. and Bayon, J.J.G., 2005. "A parametric study of vortex generators in compact heat exchanger with finned elliptical tubes". In: *6th World Conference on Experimental Heat Transfer, Fluid Mechanics and Thermodynamics (18-22 Abril 2005), 2005, Matsushima - Japão. Proceedings of the 6th World Conference on Experimental Heat Transfer, Fluid Mechanics and Thermodynamics*, pp. 1–8.
- Yanagihara, J.I. and Torii, K., 1992. "Enhancement of laminar boundary layer heat transfer by a vortex generator". *JSME International Journal*, Vol. 35, No. 3, pp. 400–405.

## 8. RESPONSIBILITY NOTICE

The authors are solely responsible for the printed material included in this paper.